A&A manuscript no.
(will be inserted by hand later)
Your thesaurus codes are:
12(02.01.2;02.13.2;08.06.2;09.10.1;11.14.1;11.10.1)

ASTRONOMY
AND
ASTROPHYSICS

Magnetized accretion-ejection structures

IV. Magnetically-driven jets from resistive, viscous, Keplerian discs

Fabien Casse and Jonathan Ferreira

Laboratoire d'Astrophysique de l'Observatoire de Grenoble BP53, F-38041 Grenoble cedex 9, France

Received 1999 July 29/ Accepted 1999 November 24

Abstract. We present steady-state calculations of self-similar magnetized accretion discs driving cold, adiabatic, non-relativistic jets. For the first time, both the magnetic torque due to the jets and a turbulent "viscous" torque are taken into account. This latter torque allows a dissipation of the accretion power as radiation at the disc surfaces, while the former predominantly provides jets with power.

The parameter space of these structures has been explored. It is characterized by four free parameters, namely the disc aspect ratio and three MHD turbulence parameters, related to the anomalous magnetic diffusivities and viscosity. It turns out that launching cold jets from thin, dissipative discs implies anisotropic turbulent dissipation. Jets that asymptotically reach a high Alfvénic Mach number are only produced by weakly dissipative discs.

We obtained general analytical relations between disc and jet quantities that must be fulfilled by any steady-state model of cold jets, launched from a large radial extension of thin discs. We also show that such discs cannot have a dominant viscous torque. This is because of the chosen geometry, imposing the locus of the Alfvén surface.

Some observational consequences of these cold magnetized accretion-ejection structures are also briefly discussed.

Key words: Accretion, accretion discs – Magnetohydrodynamics (MHD) – Stars: formation – ISM: jets and outflows – Galaxies: nuclei – Galaxies: jets

1. Cold jets from Keplerian accretion discs

Jets of plasma are observed around all young stellar objects of low mass, some galactic objects and active galactic nuclei (see the review of Livio 1997 and references therein). These jets share common properties, namely a high degree of collimation and (at least in some objects) evidences of interrelations with an underlying accretion disc (Hartigan et al. 1995, Serjeant et al. 1998). A category of very promising models explaining both galactic and extragalactic jets rely on the interaction between the accretion disc and a large scale magnetic field (for an alternative view see Lery et al. 1999). The field extracts angular momentum from the disc, thereby allowing accretion and drives the jet. This magnetized jet will be naturally self-collimated provided a large enough current is asymptotically maintained (Chan & Henriksen 1980, Heyvaerts & Norman 1989).

Following Blandford & Payne (1982) (hereafter BP82) there have been numerous studies of magnetized jet dynamics, with prescribed boundary conditions at the disc surface. As a result, the conviction grew that jets are indeed magnetized, but the question of their launching remained open. Indeed, if jets are expected to carry away a substantial fraction of the disc angular momentum, then a precise treatment of disc-jet interrelations must be done. In particular, no standard accretion disc (Shakura & Sunyaev 1973) could be used as a proper boundary condition. Hereafter, we call magnetized accretion-ejection structure (MAES), an object where accretion and ejection are interdependent.

In a series of papers (Ferreira & Pelletier 1993, Ferreira & Pelletier 1995, Ferreira 1997, hereafter FP93, FP95 and F97, respectively), such structures were investigated using two simplifying assumptions: (1) jets are cold, i.e. enthalpy plays no role in their energetics; (2) the magnetic torque due to the jets is dominant. Only geometrically thin accretion discs (Keplerian) were studied, the turbulent "viscous" torque being simply disregarded. In fact, these assumptions are common to all theoretical works dealing with the connection between accretion discs and jets (e.g. Königl 1989, Wardle & Königl 1993, Li 1995, Li 1996).

Thanks to a self-similar formulation allowing to take into account all dynamical terms, a smooth transition between the resistive accretion disc and the ideal MHD jet was achieved. The necessary conditions for steadily launching cold jets were thereby obtained. It was shown that an equipartition field is required, i.e. a magnetic energy density close to the thermal energy density (on the disc midplane). Moreover, the vertical gradient of plasma pressure is the only force that can gently expells off matter in the resistive region, against both magnetic

Send offprint requests to: Fabien.Casse@obs.ujf-grenoble.fr

and gravitational compression. Above the disc (at typically two scale-heights), matter flows along magnetic surfaces and enthalpy is indeed negligible with respect to other energies. By this process, from 1% to 10% only of accreted mass can be ejected. Since the transition from accretion to ejection occurs at the disc surface, the parameter space is highly sensitive to any approximation made on the disc vertical equilibrium (see discussion in F97).

The energetic budget of a cold MAES is quite significantly different from that of a standard disc. Indeed, the available mechanical power is shared by radiation released at the disc surfaces and an outward MHD Poynting flux that powers the jets. But in a thin disc, all the available energy is stored as rotation. Therefore, the dominant torque dictates the form and amount of dissipation that occurs to that energy. While the viscous torque produces only dissipation, hence a local heating source, the magnetic torque produces both another reservoir of energy (outward MHD Poynting flux) and a local dissipation (Joule heating). As a consequence, a stationary MAES with a dominant magnetic torque is such that almost all the liberated power feeds the jets (FP95).

This quite obvious result has strong observational consequences. Whenever jets are observed and believed to be disc-driven, then one should observe as well a lack of emission from the inner parts of the disc. This lack could be interpretated as a "hole" (Rutten et al. 1992), corresponding to the radial extension of the magnetized disc (cold MAES). However, remember that this is a direct consequence of our assumption (2). Would it then be possible to get both a significant emission from the disc and jets?

The aim of this paper is to relax the assumption of a dominant magnetic torque, keeping however the approximation of cold jets (thin or even slim discs, but without a hot corona). In Section 2, we write down the set of local MHD equations governing the whole structure, present all relevant parameters and provide general analytical results on disc-jet interrelations. In the following Section, we describe our numerical method to solve the problem and display global solutions, from the disc midplane to the super-Alfvénic jet regime. We explore the parameter space for magnetically-driven jets from resistive and viscous discs and compare our results to other models. We then conclude by summarizing our findings in Section 4.

2. Cold, non-relativistic MAES

2.1. General MHD equations

Our MAES is composed of an accretion disc settled around a central mass M_* (compact object or young star) and threaded by a large-scale magnetic field. The presence of such a field could be explained by two different phenomena: advection of interstellar magnetic field and/or local magnetic field generation by a disc dynamo (Pudritz 1981, Khanna & Camenzind 1994, Torkelsson & Brandenburg 1994, Rüdiger et al. 1995). Although a quadrupolar topology often arises from these studies, it must be kept in mind that (i) they are kinematic, hence not taking into account the magnetic feedback on the plasma motion (see Yoshizawa & Yokoi 1993) and (ii) neglect a possible primordial field that could have been advected along with the flow. Thus, it is quite difficult to infer from these works what would be the final magnetic topology in a realistic accretion disc. Moreover, it has been shown that under restricted conditions, a quadrupolar topology could produce jets from a Keplerian accretion disc, although much less powerful than those from a bipolar topology (see F97, Appendix A). We will thus assume here a bipolar topology for the disc magnetic field.

The whole MAES is described in a non-relativistic framework, so there is a limitation of our calculations when applied to the central parts of an accretion disc around compact objets. However, we are primarily interested in the interrelations between the disc and its jets. Thus, we only need to verify that matter remains sub (or even midly) relativistic close to the disc (i.e., until the Alfvén point). We neglect the disc self-gravity with respect to the gravitational field produced by the central mass and look for axisymmetric, stationnary solutions.

Thanks to axisymmetry, the vectorial quantities expressed in cylindrical coordinates (r, ϕ, z), can be decomposed into poloidal and toroidal components, e.g. $\mathbf{u} = \mathbf{u}_p + \Omega r \mathbf{e}_\phi$ and $\mathbf{B} = \mathbf{B}_p + B_\phi \mathbf{e}_\phi$. A bipolar configuration allows us to describe the poloidal magnetic field as

$$\mathbf{B}_p = \frac{1}{r}\nabla a \times \mathbf{e}_\phi \ , \tag{1}$$

where $a(r,z)$ is an even function of z and $a = constant$ describes a surface of constant magnetic flux ($a = rA_\phi$, A_ϕ being the toroidal component of the potential vector). The following set of equations describes a non-relativistic MAES (FP93):

– Mass conservation

$$\nabla.\rho\mathbf{u} = 0 \tag{2}$$

– Momentum conservation

$$\rho\mathbf{u}.\nabla\mathbf{u} = -\nabla P - \rho\nabla\Phi_G + \mathbf{J}\times\mathbf{B} + \nabla.\mathbf{T} \tag{3}$$

– Ohm's law and toroidal field induction

$$\eta_m J_\phi \mathbf{e}_\phi \ = \ \mathbf{u_p}\times\mathbf{B_p} \tag{4}$$

$$\nabla.(\frac{\nu'_m}{r^2}\nabla r B_\phi) \ = \ \nabla.\frac{1}{r}(B_\phi\mathbf{u}_p - \mathbf{B}_p\Omega r) \tag{5}$$

where ρ is the density of matter, P the thermal pressure, $\Phi_G = -GM_*/(r^2+z^2)^{1/2}$ the gravitational potential, $\mathbf{J} = \nabla\times\mathbf{B}/\mu_o$ the current, $\mathbf{T}$ the "viscous" stress tensor (Shakura & Sunyaev 1973), $\nu_m = \eta_m/\mu_o$ and ν'_m the (anomalous) poloidal and toroidal magnetic diffusivities. All transport coefficients appearing in the above set of equations, namely ν_m, ν'_m and ν_v ("viscosity", contained in $\mathbf{T}$), are assumed to be of turbulent origin.

Energy conservation is not self-consistently solved here (see the discussion in FP95). Since jets are cold, the precise way energy is transferred from the disc midplane to the jet plays no dynamical role. We can therefore freely specify the temperature profile. While previous works assumed isothermal magnetic surfaces, we will here use an adiabatic equation

$$P = K(a)\rho^\gamma \ , \tag{6}$$

where $\gamma = \frac{5}{3}$ for a monoatomic gas and $K(a)$ (related to the specific entropy) is conserved along each field line. Finally, in order to close the system, we use the perfect gas law

$$P = nk_B T \tag{7}$$

where T is the temperature of the plasma, k_B the Boltzmann constant and $n = \rho/m_p$ (m_p being the proton mass).

2.2. Relevant disc parameters

Taking into account all dynamical effects appearing in Eq. (2) to (7) is costly, for it results in quite a large number of dimensionless parameters. However, thanks to various constraints, only four of them are really free (but the parameter space of a cold MAES remaining to be spanned is large, see Sect. 3.3). Below, we list all the relevant parameters of a cold MAES.

The strength of the magnetic field in the disc is measured by

$$\mu = \left. \frac{B^2}{\mu_o P} \right|_{z=0} . \tag{8}$$

This parameter cannot be much smaller than unity for the disc would become prone to shearing instabilities (Balbus & Hawley 1991). In the present work however, we always find μ of order unity (rough equipartition).

The efficency of ejection, defined as

$$\xi = \frac{d \ln \dot{M}_a}{d \ln r} \tag{9}$$

is the key parameter linking accretion to ejection (mass conservation). For $\xi = 0$ we obviously have a standard disc, whereas a typical value for cold MAES is 10^{-2}. This parameter is strongly constrained by both the disc vertical equilibrium (minimum value of ξ) and the steady production of super-Alfvénic jets (maximum value, F97). This local ejection efficency is actually related to the magnetic flux distribution. When the magnetic flux scales as a power law of index β (i.e., $\beta = d \ln a / d \ln r_o$ is a constant), the following scaling must be fulfilled in a Keplerian disc: $\beta = 3/4 + \xi/2$ (note that BP82 used $\beta = 3/4$).

The (effective) magnetic Reynolds number, defined as

$$\mathcal{R}_m = \left. \frac{r u_r}{\nu_m} \right|_{z=0} = 2 - \beta + \frac{r^2}{\beta l^2} \tag{10}$$

where

$$\frac{a(r, z=0)}{l^2} = - \left. \frac{\partial^2 a}{\partial z^2} \right|_{z=0} ,$$

is a direct measure of the bending of the magnetic field lines at the disc midplane (where, from Eq. (4), one gets the right handside of the above equation). In previous studies, $\mathcal{R}_m$ was always of order ε^{-1}, hence providing a large amount of toroidal current at the disc midplane (FP95, F97). This current induces a large radial component of the magnetic field, such that $B_r \gtrsim B_z$ at the disc surface. This is the required bending for magnetically launching cold material (BP82). However, another situation with a much smaller $\mathcal{R}_m$ ($> 2 - \beta$) could still lead to cold ejection, provided there is an extra source of toroidal current at the disc surface.

The ratio of the magnetic torque due to the jet to the turbulent "viscous" torque at the disc midplane, namely

$$\Lambda = \left. \frac{(\mathbf{J} \times \mathbf{B})_\phi}{(\nabla . \mathbf{T})_\phi} \right|_{z=0} , \tag{11}$$

could, in principle, range from zero (standard disc) to infinity (all previous studies on magnetized accretion disc have neglected the viscous torque). Note that by "viscous" torque, we mean a radial transport of angular momentum. This "viscous" transport could originate from MHD instabilities, i.e. fluctuations of small scale magnetic fields (Stone et al. 1996).

The toroidal magnetic field at the disc surface is measured by

$$q = - \frac{h}{B_o} \left. \frac{\partial B_\phi}{\partial z} \right|_{z=0} \tag{12}$$

The shearing of the magnetic configuration is related to the current density flowing at the disc midplane and thus depends on the global electric circuit. This parameter was found to be of order unity for strongly bent poloidal field (i.e., $B_\phi \sim B_r \sim B_z$ at the disc surface, F97).

All above parameters are determined by physical constraints. Below, we present the parameters that remain free, one geometrical and three related to the MHD turbulence (ν_m, ν'_m, ν_v).

(i) The first parameter is the disc aspect ratio

$$\varepsilon = \frac{h(r)}{r} \tag{13}$$

where $h(r)$ is the local disc vertical (pressure) scale height. Having no energy equation, this parameter remains free and ε is a constant all over the magnetized disc (FP93). With our treatment, we are able to keep all terms in the equations. Therefore, we do not use the usual approximation $\varepsilon \ll 1$. In fact, solutions will be obtained for thin ($\varepsilon = 0.01$) to slim ($\varepsilon = 0.1$) discs.

(ii) The second parameter measures the strength of the MHD turbulence

$$\alpha_m = \left. \frac{\nu_m}{V_A h} \right|_{z=0} \tag{14}$$

where V_A is the Alfvén speed. If one requires stability against resistive instabilities (naively, $\tau_\nu = h^2/\nu_m \lesssim \tau_A = h/V_A$), one gets α_m of order unity.

(iii) The third parameter is the magnetic Prandtl number

$$\mathcal{P}_m = \left. \frac{\nu_v}{\nu_m} \right|_{z=0} \tag{15}$$

which measures the ratio of the "viscosity" to the poloidal magnetic diffusivity at the disc midplane. This parameter plays an important role in the angular momentum equation, which writes at the disc midplane

$$\mathcal{P}_m (1 + \Lambda) = \mathcal{R}_m . \tag{16}$$

Our usual understanding about turbulence would impose $\mathcal{P}_m$ of order unity (Pouquet et al. 1976). If this remains true in a MAES, there is a strong link between the dominant torque (Λ) and the magnetic field curvature ($\mathcal{R}_m$): strongly bent fields ($\mathcal{R}_m \sim \varepsilon^{-1}$) extract all disc angular momentum. The global energy budget of a cold MAES (with $\varepsilon \ll 1$) reads

$$P_{lib} \simeq 2 P_{rad} + 2 P_{MHD} , \tag{17}$$

where P_{lib} is the liberated mechanical power, P_{rad} the disc luminosity and P_{MHD} the outward MHD Poynting flux. The liberated power is $P_{lib} \lesssim P_{acc} \equiv GM_* \dot{M}_{ae}/2r_i$, where r_i is the disc inner radius and $\dot{M}_{ae}$ is the accretion rate at the disc outer edge r_e (FP95). Using the disc angular momentum conservation gives

$$\frac{2P_{rad}}{P_{lib}} \simeq \frac{1}{1+\Lambda}$$
$$\frac{2P_{jet}}{P_{lib}} = \frac{\Lambda}{1+\Lambda} \ . \tag{18}$$

Thus, a stationary MAES with $\mathcal{P}_m \sim 1$ and a dominant magnetic torque is such that only a fraction h/r of the total power is released as radiation. However, for the purpose of a general investigation, we will keep $\mathcal{P}_m$ free in this paper.

(iv) The last parameter measures the anisotropy of the magnetic diffusivities

$$\chi_m = \left. \frac{\nu_m}{\nu'_m} \right|_{z=0} \tag{19}$$

at the disc midplane. An isotropic turbulent dissipation would be described with χ_m of order unity. However, we expect the leading instabilities triggered inside the MAES to produce enhanced dissipation of the toroidal field, thus providing $\chi_m < 1$.

2.3. *Launching jets from Keplerian discs*

In order to eject matter from the disc, a necessary condition is that the magnetic torque changes its sign at the disc surface. Indeed, it brakes the matter in the disc midplane and both angular momentum and energy are stored in the magnetic field. Above the disc, angular momentum and energy must be given back to matter for launching a jet, namely $(\mathbf{J} \times \mathbf{B}).\mathbf{e}_\phi > 0$ at $z = h$. The toroidal component of the Lorentz force is mainly governed by the behaviour of the radial current density, which is in turn controled by the induction equation (5). Integrated vertically, this equation gives

$$\eta'_m J_r = \eta'_o J_o + r \int_0^z dz \mathbf{B}_p.\nabla\Omega - B_\phi u_z \ . \tag{20}$$

The last term (field advection) is negligible in the resistive disc but will exactly balance the differential rotation effect in the ideal MHD region. The change of sign of the magnetic torque implies that the radial current density *must* decrease on a disc scale height. After some approximations[1], the necessary condition for launching a jet is found to be

$$\Lambda = \frac{3\chi_m}{\alpha_m^2 \varepsilon \mathcal{P}_m} \ . \tag{21}$$

This very important relation does not allow much freedom in thin discs. Indeed, for conventional values of the turbulence parameters ($\alpha_m \sim \mathcal{P}_m \sim \chi_m \sim 1$), one gets $\Lambda \sim \varepsilon^{-1}$, namely a dominant magnetic torque. To enforce comparable torques ($\Lambda \sim 1$), one then must ask for either an anisotropic turbulence ($\chi_m < 1$) or a large $\mathcal{P}_m$ (or both). A fortiori, launching cold jets with $\Lambda \ll 1$ seems almost impossible. Cold jets have a tremendous influence on the disc structure. One useful quantity to evaluate is the ratio σ of the MHD Poynting flux to the kinetic energy flux,

$$\sigma_{SM} \simeq \frac{\Lambda}{\xi(1+\Lambda)} \ , \tag{22}$$

measured here right above the disc (at the slow magnetosonic point). It shows that, unless ξ is of order unity or $\Lambda \sim \xi$, the magnetic field completely dominates matter at the disc surface (i.e., $\sigma_{SM} \gg 1$).

To summarize, Λ is constrained by the very existence of a jet, $\mathcal{R}_m$ by the disc angular momentum conservation and q is an explicit functions of the other parameters:

$$q = \frac{\alpha_m}{2} \mathcal{R}_m \varepsilon \delta \mu^{-1/2} \frac{\Lambda}{1+\Lambda} \ , \tag{23}$$

with $\delta = \Omega_o/\Omega_K$, ratio of the angular velocity at the disc midplane to the Keplerian rate Ω_K (see the exact expression of δ in Eq. (46)). The two remaining disc parameters, ξ and μ, are constrained by the smooth crossing of two critical points (slow magnetosonic and Alfvén, see FP95). Thus, the present model has only four free parameters. In the next section, we show the strong links between cold jet parameters and those describing the disc. In practice however, we will impose a set of disc parameters $(\varepsilon, \alpha_m, \mathcal{P}_m, \chi_m)$ and obtain a posteriori the jet parameters.

2.4. *Relevant jet parameters*

The jet is the region where the transport coefficients are equal to zero, namely the ideal MHD medium above the disc. In this regime, mass and flux conservations combined with Ohm's law (4) provide

$$\mathbf{u}_p = \frac{\eta(a)}{\mu_o \rho} \mathbf{B}_p \tag{24}$$

where $\eta(a) = \sqrt{\mu_o \rho_A}$ is a constant along a magnetic surface and ρ_A is the density at the Alfvén point, where the poloidal velocity reaches the poloidal Alfvén velocity. The induction equation (5) becomes

$$\Omega_*(a) = \Omega - \eta \frac{B_\phi}{\mu_o \rho r} \ , \tag{25}$$

where $\Omega_*(a)$ is the rotation rate of a magnetic surface (very close to the Keplerian value). In the jet, plasma flows along a magnetic surface with a total velocity $\mathbf{u} = (\eta/\mu_o\rho)\mathbf{B} + \Omega_* r \mathbf{e}_\phi$ not parallel to the total field.

The angular momentum conservation in the jet simply writes

$$\Omega_* r_A^2 = \Omega r^2 - \frac{r B_\phi}{\eta} \tag{26}$$

where r_A is the Alfvén radius. Above the disc, the turbulent torque vanishes and only remains a magnetic accelerating torque.

The projection of the momentum conservation equation along a magnetic surface provides the Bernoulli equation

$$\frac{u^2}{2} + H + \Phi_G - \Omega_* \frac{r B_\phi}{\eta} = \mathcal{E}(a) + \Omega_*^2 r_A^2 = E(a) \ , \tag{27}$$

[1] see Appendix B of F97. In order to obtain a generalization of his expressions, replace his condition $\Gamma \simeq 1$ by $\Gamma \simeq \mathcal{R}_m \varepsilon$.

where $E(a)$ is the constant specific energy carried by the jet, H is the specific enthalpy defined as $H = \gamma P/(\gamma-1)\rho$ in the adiabatic case. Enthalpy is negligible for "cold" plasma ejection at the disc surface.

The shape of the magnetic surface is given by the jet transverse equilibrium, namely the Grad-Shafranov equation that can be written in the following form

$$(1 - m^2)J_\phi = J_\lambda + J_\kappa \ , \tag{28}$$

where the sources of current are

$$J_\lambda \ = \ \rho r \left(\frac{d\mathcal{E}}{da} + (1-g)\Omega_* r^2 \frac{d\Omega_*}{da} + g\Omega_* \frac{d\Omega_* r_A^2}{da} \right)$$
$$J_\kappa \ = \ r\frac{B_\phi^2 - m^2 B_p^2}{2\mu_o}\frac{d\ln \rho_A}{da} + m^2 \frac{\nabla a}{\mu_o r}.\nabla \ln \rho$$

Here, $m^2 = u_p^2/V_{Ap}^2$ is the Alfvén Mach number and $g = 1 - \Omega/\Omega_*$ (Pelletier & Pudritz 1992, hereafter PP92).

We choose to use the usual jet parameters as defined by BP82. Equation (24) allows to define a mass load parameter

$$\kappa = \eta \frac{\Omega_o r_o}{B_o} \ , \tag{29}$$

where the subscript o defines quantities at the disc midplane. This dimensionless parameter describes the mass flux per magnetic flux unit ($d\dot{M}_j/da = 2\pi\eta/\mu_o$), thus it is constrained by the disc vertical equilibrium.

The total specific angular momentum, defined by

$$\lambda = \frac{\Omega_* r_A^2}{\Omega_o r_o^2} \simeq \frac{r_A^2}{r_o^2} \tag{30}$$

provides a measure of the magnetic lever arm acting on the disc, i.e. a measure of the Alfvén radius r_A. In the case where all the MHD Poynting flux is converted into jet kinetic power, the magnetic lever arm parameter uniquely determines the jet terminal velocity

$$u_{p,max} = \Omega_o r_o (2\lambda - 3)^{1/2} \ . \tag{31}$$

The asymptotic jet behaviour is strongly influenced by another normalized quantity. This last jet parameter ("fastness" parameter) is a direct measure of how fast the magnetic rotator is (Michel 1969, PP92, F97, Lery et al. 1998)

$$\omega_A = \frac{\Omega_* r_A}{V_{Ap,A}} \ . \tag{32}$$

PP92 showed that super-Alfvénic jets require ω_A bigger than unity. This subtle parameter links rotation of the magnetic surface to poloidal motion. In our calculations, it is intimately related to the MHD power still available at the Alfvén surface. For ω_A bigger than but close to unity (or $g_A < 1/2$), matter reaches the Alfvén surface at the expense of all the MHD Poynting flux (no more current available) but recollimation takes place just after it. For larger ω_A (typically bigger than 1.4, or $g_A > 1/2$), a large amount of current is still available and the jet propagates much farther away before recollimation occurs (F97). The "fastness" parameter ω_A determines also the magnetic geometry at the Alfvén surface, both pitch ($\arcsin(-B_\phi/B_p)$) and opening ($\theta = \arccos(B_z/B_p)$) angles. The larger ω_A, the larger these angles (centrifugal effect stronger than the hoop stress), providing a subsequent large widening of the jet. The fastness parameter ω_A is directly proportional to the toroidal field at the disc surface q (see below). This parameter did not explicitely appear in BP82, but it was hidden in the initial angle of field lines at the disc surface (the larger angle, the larger B_ϕ).

In usual treatments of MHD jets, where the disc is a mere boundary condition, κ is fixed by the regularity condition at the slow point whereas λ is fixed by the Alfvénic condition for a given ω_A. In our treatment, all these cold jet parameters are completely fixed by the set of disc parameters. Using ideal MHD equations, mass conservation and angular momentum conservation, we get

$$\lambda \ = \ 1 + \frac{\sigma_{SM}}{2} \simeq 1 + \frac{\Lambda}{2\xi(1+\Lambda)}$$
$$\kappa \ = \ \frac{q}{\lambda - 1} \simeq \alpha_m(\mathcal{P}_m\varepsilon + \frac{3\chi_m}{\alpha_m^2})\delta\xi\mu^{-1/2} \tag{33}$$
$$\omega_A \ \simeq \ q\frac{\lambda^{3/2}}{\lambda - 1}\frac{\sin(\phi_A - \theta_A)}{\sin\phi_A}$$

where ϕ_A is the angle between the Alfvén surface and the vertical axis, and θ_A is the opening angle estimated at the Alvénic transition. This angle θ_A is implicitly determined by the Grad-Shafranov equation (see Appendix A). The angle ϕ_A is imposed by the chosen geometry of the Alfvén surface. Note that this last expression is valid for conical Alfvén surfaces (see Appendix B), a geometry which arises naturally when the above parameters vary slowly across the jet. Rewriting the last expression as

$$\omega_A \sim \alpha_v \varepsilon \Lambda \frac{\lambda^{3/2}}{\lambda - 1}\frac{\sin(\phi_A - \theta_A)}{\sin\phi_A} \ , \tag{34}$$

where α_v is the usual alpha parameter for turbulent viscosity (Shakura & Sunyaev 1973), and using the necessary condition for super-Alfvénic jets ($\omega_A > 1$) provides

$$\Lambda > \frac{\lambda - 1}{\lambda^{3/2}}\frac{1}{\alpha_v\varepsilon} \ . \tag{35}$$

This is a strong constraint on the underlying accretion process. A dominant viscous torque ($\Lambda < 1$) would then require either (1) α_v smaller than unity but huge magnetic lever arms, namely $\lambda > \varepsilon^{-2}$, or (2) $\alpha_v > \varepsilon^{-1}$. Whether the last condition is clearly unphysical, the former remains open at this stage.

3. Global solutions from disc to jets

3.1. Numerical approach

3.1.1. The self-similar ansatz

In order to have a global solution for a MAES, we need to solve the whole set of MHD equations (2) to (7). Because these equations are highly non-linear partial differential equations, we use a variable separation method that greatly simplifies the resolution. Self-similarity allows us to write all the quantities like

$$Q(r,z) = Q_e \left(\frac{r}{r_e}\right)^{\alpha_Q} f_Q(x) \tag{36}$$

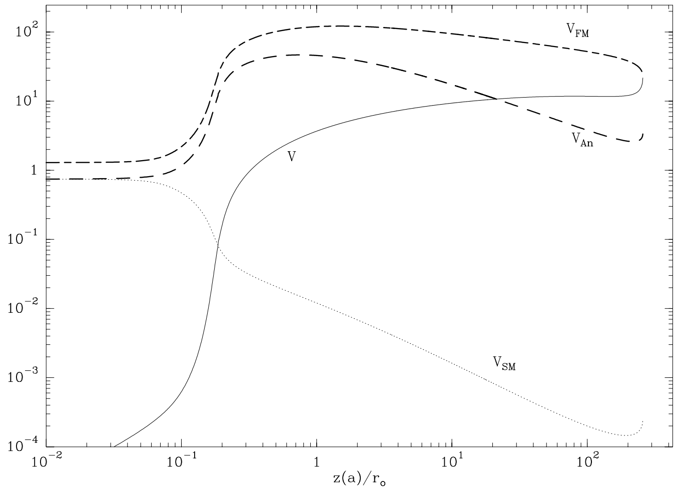

Fig. 1. Characteristic velocities along a magnetic surface, normalized to the local disc sound speed $\Omega_K h_o$: slow and fast magnetosonic velocities V_{SM} and V_{FM}, critical plasma velocity $V = \mathbf{u}.\mathbf{n}$ ($\mathbf{n}$ is the relevant direction of wave propagation, FP95) and the Alfvén velocity V_{An} (note that $V = V_{An}$ is equivalent to $u_p = V_{Ap}$). These curves describe the MAES presented in Fig. 2. However, the behaviour is common to all self-similar, cold jets from Keplerian discs obtained so far. Note that the jet is super-fast in the usual sense ($u_p > V_{FM}$, F97).

where $x = z/h(r)$ and r_e is the outer radius of the magnetized disc. By doing this, we obtain a set of ordinary differential equations acting on f_Q where we can consider all terms of each equation. The values of the coefficents α_Q are given by FP93. The magnetic flux is written

$$a(r,z) = a_e \left(\frac{r}{r_e}\right)^{\beta} \psi(x) \tag{37}$$

To obtain the variation of any quantity Q along a magnetic surface, we just have to write

$$Q(x) = Q_o \psi^{-\alpha_Q/\beta}(x) f_Q(x) \tag{38}$$

where x must be understood here as a curvilinear abscissa along the magnetic surface. In fact, we find more convenient to choose as a curvilinear variable $z(a)/r_o = \varepsilon x \psi^{-1/\beta}(x)$, since it directly provides a physical scale once r_o is chosen.

3.1.2. Turbulent transport coefficients

In the self-similar framework, only the vertical variation of the turbulent transport coefficents must be prescribed. Since these anomalous coefficents are expected to arise from an MHD turbulence triggered inside the disc, we assume that the magnetic diffusivities ν_m and ν'_m decrease on a disc scale-height. We therefore used a Gaussian law for their vertical profile.

The same issue appears for the turbulent "viscous" torque, which is responsible for the radial transport of angular momentum. Following the above arguments, the corresponding turbulent viscosity ν_v would also decrease on a disc scale-height. However, we must take care to conserve the total disc angular momentum. For this purpose, we write the angular momentum conservation equation as

$$\nabla.(\rho \Omega r^2 \mathbf{u}_p - \frac{r B_\phi}{\mu_o}\mathbf{B}_p - r\boldsymbol{\tau}) = 0 \tag{39}$$

where we used

$$\frac{1}{r}\nabla.(r\boldsymbol{\tau}) = (\nabla.\mathbf{T}).\mathbf{e}_\phi \quad \text{and} \quad \boldsymbol{\tau} = \begin{pmatrix} \tau_r \\ 0 \\ \tau_z \end{pmatrix}$$

MHD discs launching cold jets have comparable radial and vertical gradients of the angular velocity Ω, hence providing comparable components $T_{r\phi}$ and $T_{z\phi}$ of the turbulent stress tensor. Thus, prescribing the vertical profile of the poloidal components of $\boldsymbol{\tau}$ (instead of the torque itself or the viscosity), insures the conservation of the total angular momentum. Because the turbulent *torque* must be an even function of x, we use a $\exp(-x^4)$ law intead of a simple Gaussian law. The resulting turbulent torque remains always negative in the disc and decreases on a disc scale height.

3.2. Numerical results

With a given set of disc parameters $(\varepsilon, \alpha_m, \mathcal{P}_m, \chi_m)$, we integrate the set of ordinary differential equations step by step with respect to the self-similar variable $x = z/h(r)$. The transition between the resistive, viscous disc and the ideal MHD medium occurs smoothly above the disc surface.

The determinant appearing in the set of ideal MHD equations vanishes when the critical plasma velocity is equal to the phase velocity of a typical wave of the medium: slow magnetosonic (SM), Alfvén (A) and fast magnetosonic (FM) waves. As already shown by many authors (e.g. BP82 and FP95 for the exact self-similar expressions of these velocities), the expressions of these velocities are modified by self-similarity. The slow point is mostly related to the vertical velocity, the Alfvén to the poloidal one, whereas the fast is related to the radial velocity.

For given $(\varepsilon, \alpha_m, \mathcal{P}_m, \chi_m)$, the smooth crossing of these points is allowed by fine-tuning two parameters, namely μ and ξ. For the slow point, the strength of the magnetic field μ must be equal to a critical value μ_c. If $\mu < \mu_c$ the density profile is flatter, leading to a fall of the vertical speed of matter, whereas if $\mu > \mu_c$, the magnetic field pinches too strongly the disc, forbidding matter to leave the disc. The crossing of the Alfvén point is controled by the efficency of ejection ξ. If $\xi > \xi_c$ the magnetic field lines are too much opened because of an overwhelming centrifugal effect. This leads to $\Omega r^2 > \Omega_* r_A^2$, that is $B_\phi > 0$ and the structure is non-steady. On the contrary, $\xi < \xi_c$ leads to an unphysical closing of the magnetic surfaces due to the magnetic tension. For each attempt to cross the Alfvén point by fine-tuning ξ, we must find again the critical μ.

As in F97, all trans-Alfvénic solutions presented here do not cross the last critical point, the fast magnetosonic one. The numerical integration stops at exactly the location of this point

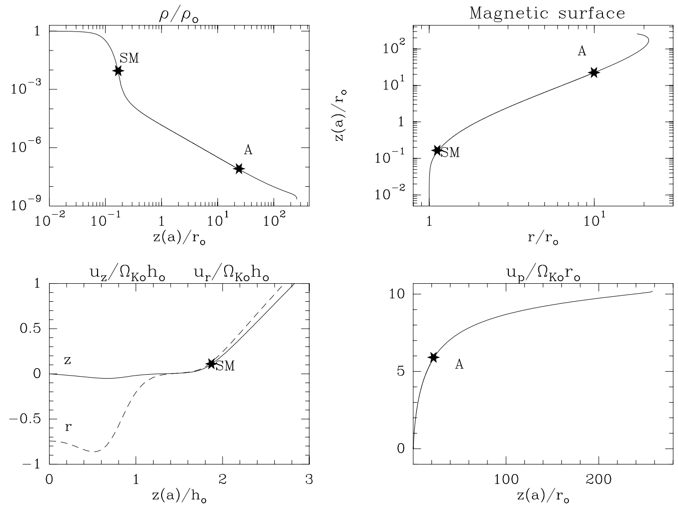

Fig. 2. Typical solution from a dissipative disc (Λ = 2.43) with $\varepsilon = 0.1$, $\alpha_m = 1$, $\mathcal{P}_m = 3.2$ and $\chi_m = 0.259$. All quantities are shown along a magnetic poloidal line, anchored on a radius r_o. The density (upper left pannel) is normalized to the density ρ_o at the disc midplane and jet poloidal velocity (lower right pannel) to the Keplerian velocity. Stars show the location of the slow-magnetosonic (SM) and Alfvén (A) critical points. The magnetic surface (upper right pannel) presents the usual recollimating behaviour once all MHD power has been converted into kinetic power (plateau in the poloidal velocity). The lower left pannel shows both radial and vertical components of the plasma velocity inside the disc, normalized to the sound speed. The transition between the resistive disc and ideal MHD jet occurs above the disc surface ($z/h \sim 1.6$), where both components become comparable.

(see Fig. 1). The meeting of this last point is unavoidable provided the numerical integration is done sufficiently far. Actually, it seems inherent to self-similar solutions that the crossing of the three critical points is impossible (see discussion in F97).

Only high-ω_A jets propagate much farther away than the Alfvén point, widening a lot ($r_\infty \gg r_A$) and reaching large asymptotic Alfvénic Mach numbers ($m_\infty^2 \gg 1$). We label these jets as being powerful. Such jets are produced whenever the initial MHD Poynting flux is high, namely when the radial current density is large on the disc midplane. Thus, a high value of q (close to unity) is required for cold jets launched from a large radial extension in the disc. Then, such jets exert a large torque on the disc midplane, thereby producing a large accretion velocity.

For a small poloidal magnetic diffusivity, the poloidal field will tend to be strongly bent by the accretion flow, eventually providing a large magnetic Reynolds number. In this case, the turbulent torque becomes negligible and all the available power goes into the jet. Not much power is finally radiated at the disc surfaces. Requiring both high-ω_A, cold jets and a dissipative disc is quite a difficult task, that can however be achieved in two different (though costly) ways.

Equation (16) shows that for a magnetic Prandtl number $\mathcal{P}_m$ of order unity there is a strong link between the magnetic configuration ($\mathcal{R}_m$) and the magnetic torque (Λ). Increasing the magnetic diffusivity only (α_m), so that the field lines remain almost vertical inside the disc ($\mathcal{R}_m \sim 1$), leads to comparable torques. Therefore, a comparable amount of energy is released as radiation and MHD Poynting flux. The other possibility consists on increasing the magnetic Prandtl number only ($\mathcal{P}_m > 1$). In this way, the effects of the turbulent viscosity are enhanced so that comparable torques can still be achieved, even with a strongly bent poloidal magnetic field ($\mathcal{R}_m \sim \varepsilon^{-1}$).

Actually, it is noteworthy that using the Shakura-Sunyaev prescription for the viscosity ($\nu_v = \alpha_v \Omega_K h^2$) gives

$$\alpha_v = \alpha_m \mathcal{P}_m \mu^{1/2} . \quad (40)$$

Thus, both ways of obtaining dissipative discs producing high-ω_A jets imply an increase of the viscosity parameter α_v.

Figure 2 illustrates a typical dissipative solution, described with the set of parameters $(\varepsilon, \alpha_m, \mathcal{P}_m, \chi_m) = (0.1, 1, 3.2, 0.259)$. This solution is in the upper right side of the parameter space represented in Fig. 3. It corresponds to a dissipative disc ($\Lambda = 2.43$, 29% of the total mechanical power being released as radiation) and high-ω_A jets. The resulting set of jet parameters is $(\kappa, \lambda, \omega_A) = (5\ 10^{-3}, 78, 1.44)$.

Inside the disc, both the radial and vertical components of the plasma velocity are negative. Matter is accreting towards the central object and slightly converging toward the disc midplane. The transition from accretion to ejection occurs at the disc surface, where all dynamical terms are comparable. At the surface, the steep decrease of the density profile ($\rho^+ = \rho(h) \sim \varepsilon\rho_o$, where ρ_o is the density at the disc midplane) goes along with a typical outflow velocity

$$u_z^+ \simeq u_o \xi . \quad (41)$$

This transition occurs in still resistive and viscous upper layers, where the magnetic torque azimuthaly accelerates the plasma. Farther out, both the decrease of the transport coefficients and the Lorentz force itself, enforce plasma to flow along magnetic surfaces. Once in this ideal MHD regime, the flow encounters the first critical point (SM).

As previously said, the asymptotic jet behaviour is exactly the same as in F97. Plasma always achieves its maximum velocity (mostly vertical), almost all initial MHD Poynting flux being finally converted into kinetic energy (Fig. 2). Jets become super fast-magnetosonic in the conventionnal sense, namely $u_p > V_{FM} \simeq V_{A\phi}$ ($B_\phi \gg B_p$). From this point on, both the centrifugal force and total pressure gradient cannot overcome the hoop stress. This leads to a recollimation of the magnetic surface (negative opening angle), until the last critical point is finally met (Fig. 1). The maximum radius achieved depends mostly on ω_A (see Fig. 12 in F97).

High-ω_A jets from a dissipative disc were obtained here by increasing the magnetic Prandtl number. In this particular case, we obtained a phenomenological viscosity parameter $\alpha_v \simeq 2.2$, bigger than unity. This is problematic since one usually expects a turbulence which is both subsonic and with a correlation length smaller than the disc scale height (hence $\alpha_v < 1$). Alternatively, we did find a dissipative solution with $\alpha_v = 0.27$, but the price was an increase of the MHD turbulence parameter $\alpha_m = 1.8$. It seems therefore too costly to

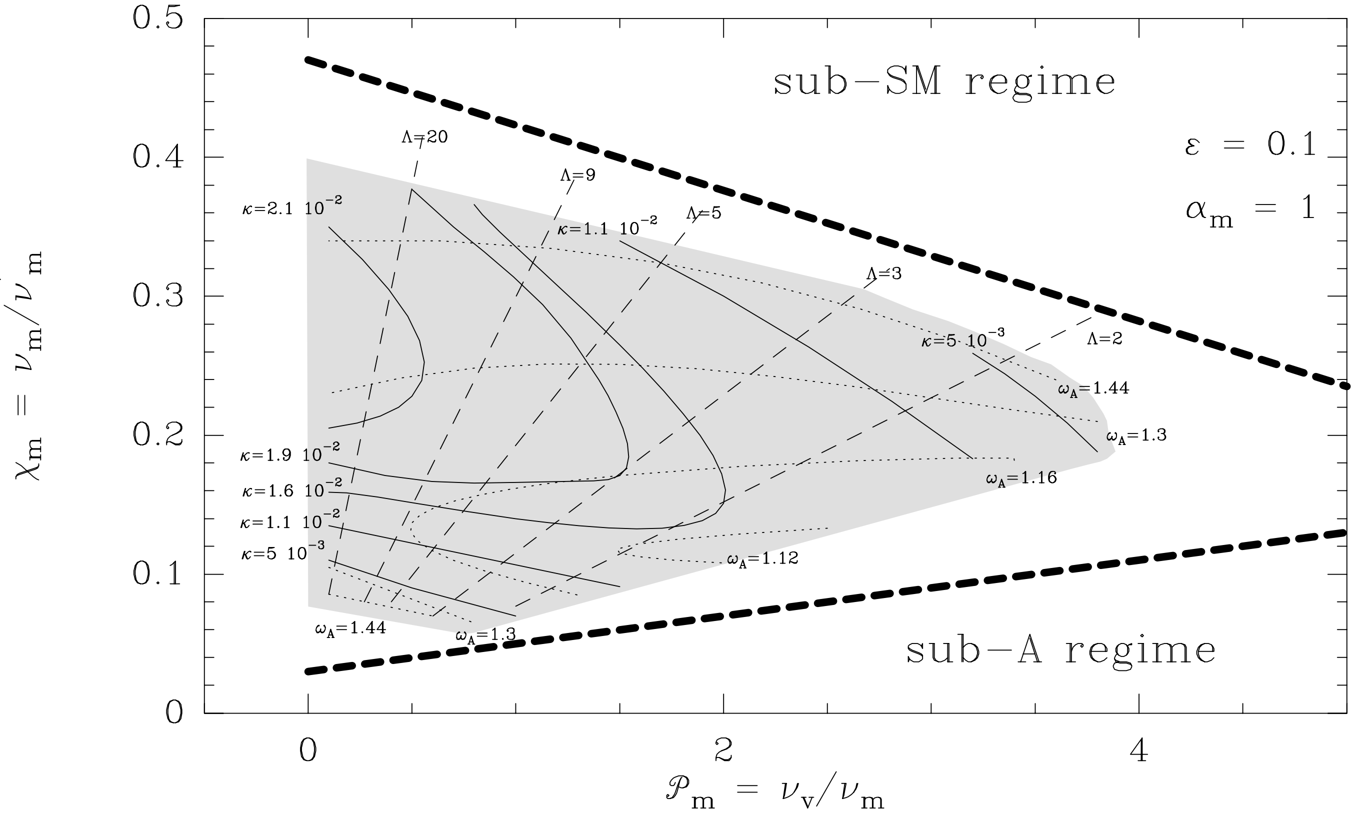

Fig. 3. Parameter space of cold, non-relativistic magnetized accretion-ejection structures for $\alpha_m = 1$ and $\varepsilon = 0.1$. The shaded area corresponds to the location where numerical solutions could be found. Thick dashed lines show theoretical limits: super-slow magnetosonic (upper limit) and super-Alfvénic (lower limit) flow. While the range in χ_m is quite narrow, the one covered by the magnetic Prandtl number is quite large (from 10^{-2} to almost 4). Levels for the corresponding jet parameters κ and ω_A are also displayed.

get both high-ω_A jets and dissipative discs. To firmly settle this issue, we scanned the parameter space of cold MAES.

3.3. Parameter space of adiabatic, cold jets from Keplerian discs

The parameter space of cold MAES is obtained by varying the set of free disc parameters $(\varepsilon, \alpha_m, \mathcal{P}_m, \chi_m)$. We choose to fix the values of both ε and α_m and represent the parameter space with the remaining parameters (Fig. 3 and 4). Numerical solutions are only found inside the shaded areas, where we also plot levels of two jet parameters ω_A and κ. This region is embedded inside a larger region (thick dashed lines), obtained by two analytical constraints.

The first constraint arises from the requirement that jets become super-slow magnetosonic. It is thus related to the disc vertical equilibrium: a too strong magnetic pinching of the disc forbids plasma to escape from it. Since plasma pressure is the only force that allows matter to be lifted from the disc, it cannot be much smaller than the vertical component of the magnetic pressure. This magnetic pressure is due to the growth of both radial and toroidal magnetic fields. Using a Taylor expansion (on z), this constraint can be written as

$$h\frac{\partial}{\partial z}\left(\frac{B_r^2 + B_\phi^2}{2B_o^2}\right) \simeq \mathcal{R}_m^2 \varepsilon^2 \frac{z}{h}\left(1 + \frac{\alpha_m^2 \Lambda^2}{4\mu(1+\Lambda)^2}\right) \leq 2 \; , \quad (42)$$

Each contribution to the magnetic compression is expected to be smaller than the one provoked by the vertical magnetic field (equipartition between plasma pressure and magnetic pressure at the disc midplane). The upper limit appearing in Fig. 3 and 4 corresponds to a necessary condition involving only the radial component, namely

$$\chi_m < \frac{\alpha_m^2}{3}(\sqrt{2} - \mathcal{P}_m \varepsilon) \; . \quad (43)$$

This Taylor expansion is however not valid in discs where the poloidal magnetic field is straight ($\mathcal{R}_m \sim 1$). In that case, there is an extra source of toroidal current at the disc surface, leading to a large bending of the poloidal field. The corresponding magnetic pressure increases with the magnetic lever arm. This is what happens in solutions located at the left lower part of Fig. 3 (high lever arms λ require tiny mass loads κ, Fig. 5).

The other constraint emerges from the requirement that jets must become super-Alfvénic. This is expressed by $\omega_A > 1$, which can be written as

$$\chi_m\left(\chi_m^2 - \frac{8\xi\mu}{9\delta}\alpha_m^2\right) > \frac{8\alpha_m^4}{27}\frac{\xi\mu\varepsilon}{\delta}\mathcal{P}_m \quad (44)$$

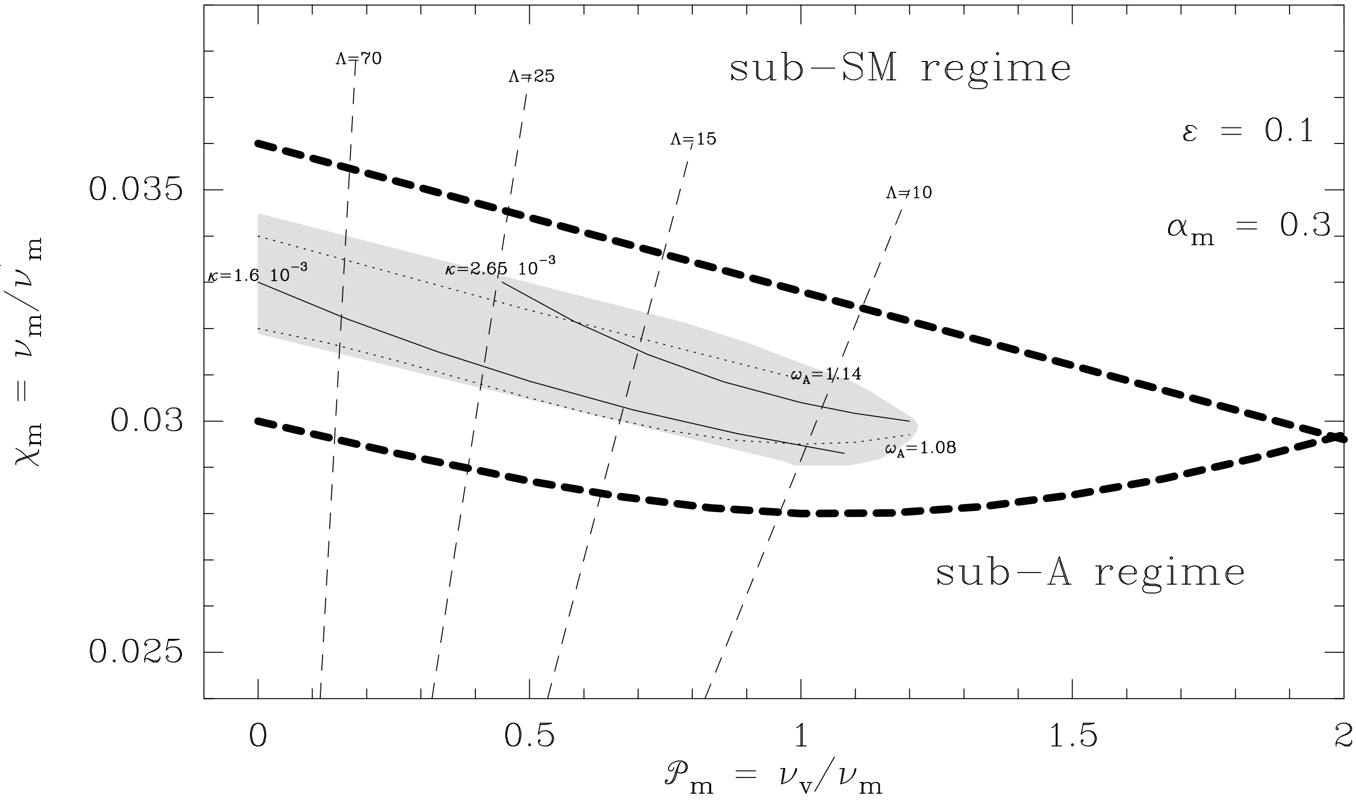

Fig. 4. Parameter space of cold, non-relativistic magnetized accretion-ejection structures for $\alpha_m = 0.3$ and $\varepsilon = 0.1$. For a smaller α_m, the region where solutions can be found is much smaller (see Fig. 3), with a magnetic Prandtl number ranging from 10^{-2} to 1.2. Here no dissipative solution could be found and jets could not reach an ω_A stronger than 1.15.

providing the lower limits in the same figures. These two constraints strongly depend on both α_m and ε.

It turns out that the above two constraints behave differentely with α_m. As a result, the parameter space shrinks considerably (upper and lower limits merging together) for decreasing α_m and widens for increasing α_m. We show in Fig. 4, the parameter space for $\alpha_m = 0.3$; the space is considerably reduced and produces no high-ω_A jet. Physically, it means that if turbulence is not strong enough, the magnetic torque will not be able to store enough angular momentum in the magnetic field (parameter q) to accelerate matter to the Alfvén surface. A much smaller mass load would avoid this problem, but this would require an overwhelming magnetic pinching and no trans-SM solution can be found for cold jets. On the other hand, α_m cannot be much bigger than unity otherwise a too strong magnetic compression due to the toroidal magnetic field will occur (Eq. (42)). Numerically, we do not found any solutions for $\alpha_m > 3$.

No solution with a dominant viscous torque ($\Lambda \ll 1$) has been found. As showed in Sect. 2.4, super-A jets would require magnetic lever arms much bigger than ε^{-2}. This is impossible here because of the tremendous pinching due to the radial component of the magnetic field. Hence, both super-SM and super-A constraints merge together for decreasing torque ratios Λ. Thus, cold disc-driven jets launched from a large radial extension always carry a large fraction of the disc angular momentum ($\Lambda > 1$). Furthermore, our solutions always produced a large magnetic lever arm ($\lambda > 3$). This allows us to generalize the constraint on the maximum ejection index ξ (see Sect. 3.3.2 in F97), namely

$$\xi < \frac{\sqrt{13}-3}{4}\frac{\Lambda}{\Lambda+1} \,, \tag{45}$$

which is compatible with the numerical values found.

Only a rather small range of disc aspect ratios allows cold MAES to exist. This can be understood quite easily. While a maximum value is imposed by the disc radial equilibrium, cold jet production implies a minimum value. Indeed, the disc radial equilibrium writes at the midplane

$$\frac{\Omega_o}{\Omega_K} = \delta = \left(1 - \varepsilon^2\left[\frac{m_s^2}{2} + 2(2-\beta) + \mu\mathcal{R}_m\right]\right)^{1/2} \tag{46}$$

where

$$\begin{aligned} m_s \;&\equiv\; \frac{u_o}{\Omega_K h} = 2q\mu\frac{1+\Lambda}{\Lambda} = \alpha_v\varepsilon(1+\Lambda) \\ &=\; \alpha_m(\mathcal{P}_m\varepsilon + 3\chi_m/\alpha_m^2)\mu^{1/2} \end{aligned} \tag{47}$$

is the sonic Mach number. Deviations from Keplerian law are mainly due to the radial gradient of plasma pressure (of order ε^2) and the magnetic tension (of order $\mathcal{R}_m\varepsilon^2$). Plasma pressure alone makes it obvious that requiring the disc to rotate implies that it cannot be too thick. However, the magnetic tension, which is a slowly decreasing function of height, provides

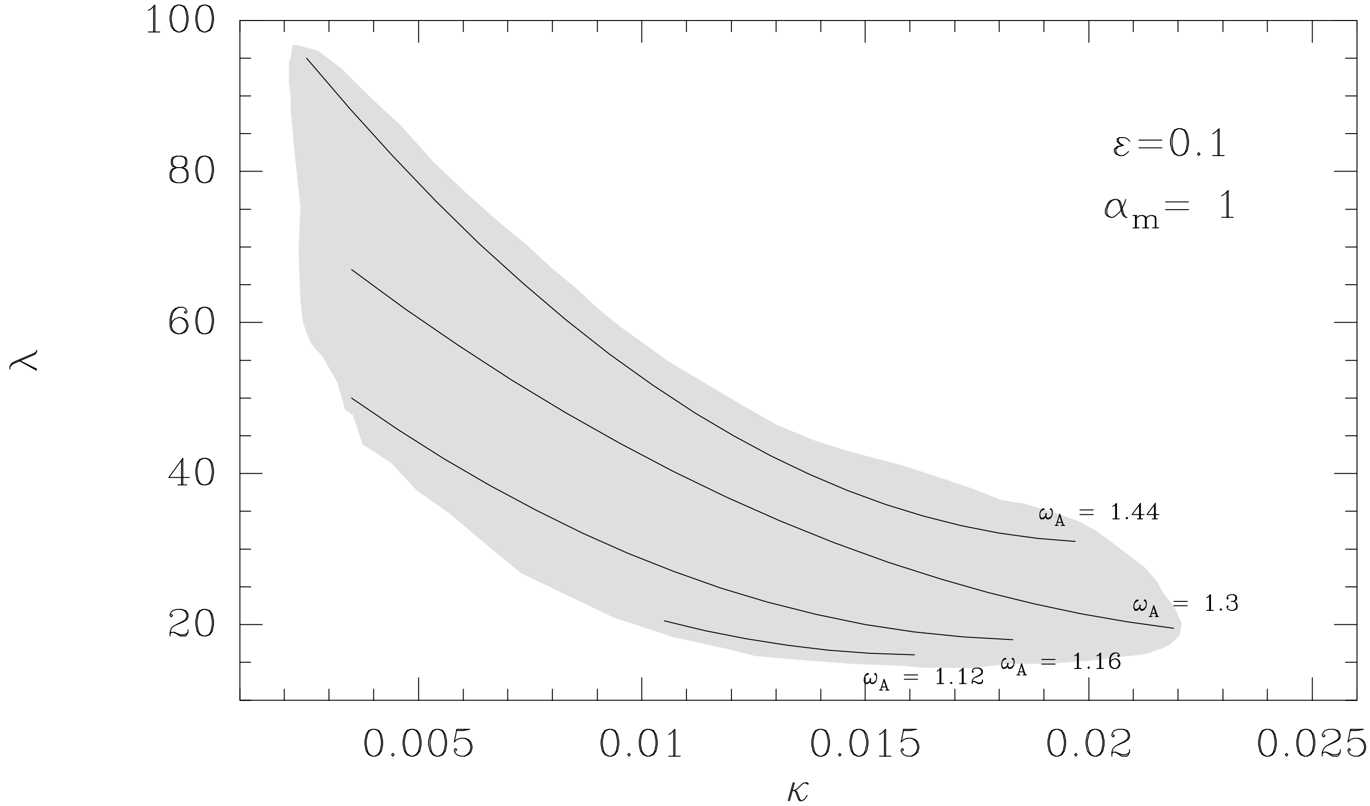

Fig. 5. Parameter space of cold, adiabatic jets from Keplerian discs with $\alpha_m = 1$ and $\varepsilon = 0.1$. It illustrates the disc parameter space in Fig. 3. The lower limit of the shaded area is imposed by the Alfvénic constraint: no trans-Alfvénic jet can be found below. The upper limit is imposed by the disc vertical equilibrium (trans-SM jet). This parameter space for jets is to be compared with those obtained by Blandford & Payne (1982), Wardle & Königl (1993) and Li (1995). Using this plot along with Fig. 3 allows to compute all other MAES parameters (ξ, μ, q).

an even stronger constraint. Indeed, as the density falls down, the magnetic support becomes more and more important and leads to no rotation (or even a negative one) for too thick discs. Numerically, we did not found solutions for $\varepsilon > 0.3$.

It is noteworthy that there is no dissipative cold MAES for discs too thin ($\varepsilon < 0.05$). This is because of the condition for launching a cold jet. Indeed, Eq. (21) implies that χ_m must be of order ε to have $\Lambda \sim 1$. But this cannot be verified for very small ε because of the trans-Alfvénic condition (44). One can easily see that the thicker disc and the more dissipative MAES.

3.4. *Can identical jets be produced from different discs?*

The complexity of Figures 3 and 4 raises the question whether identical jets could be produced from different discs. Once in ideal MHD regime, equations (24) to (28) and Eq. (6) completely determine the jet structure. The leading equation is the Grad-Shafranov equation (28), which provides the jet transverse equilibrium. In the most general case, the solution is elliptic below the Alfvén surface. This means that the sub-Alfvénic solution is completely determined once we choose the values of all relevant quantities at the Alfvén surface. In the self-similar case, the transfield equation reduces to a second order differential equation of the form

$$\frac{d^2 r}{dz^2} = \frac{\mathcal{G}}{\mathcal{F}}\left(r, \frac{dr}{dz}, z\right) \tag{48}$$

where $r(z)$ describes the shape of magnetic surfaces (Contopoulos & Lovelace 1994). Therefore, identical jet structures are produced whenever both the leading dimensionless parameters $(\kappa, \lambda, \omega_A)$ and conditions at the Alfvén point are the same. It can be shown (see Appendix B) that the locus of the Alfvén surface is given by

$$\begin{aligned} \frac{r_A}{r_o} &= \lambda^{1/2} \\ \frac{z_A}{r_A} &= \cot\phi_A = \cot\theta_A\left(1 - \frac{\omega_A}{\kappa\lambda^{3/2}\cos\theta_A}\right), \end{aligned} \tag{49}$$

where z_A is always found to be of order r_A. The magnetic configuration (opening and pitch angles) at the Alfvén point satisfies

$$\begin{aligned} \frac{B_{p,A}}{B_o} &= \kappa\frac{\lambda^{1/2}}{\omega_A} \\ \left.\frac{B_r}{B_z}\right|_A &\equiv \left.\frac{dr(z)}{dz}\right|_A = \tan\theta_A(\kappa, \lambda, \omega_A) \qquad (50) \\ \left.\frac{B_\phi}{B_p}\right|_A &= -g_A\omega_A \end{aligned} \tag{51}$$

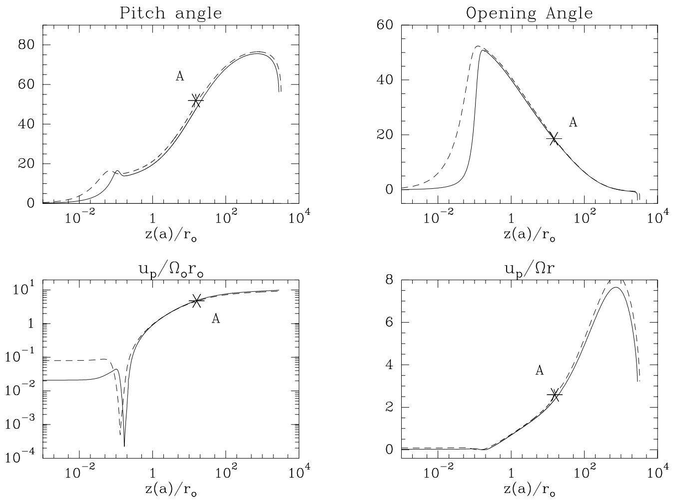

Fig. 6. Plots along a magnetic surface anchored at r_o of the principal characteristics of two MAES, with the same set of jet parameters but different disc parameters (see Sect. 3.4). One is a dissipative disc (solid line) where both torques are comparable ($\Lambda = 1.95$), whereas the second is a weakly dissipative disc (dashed line) with a much higher magnetic torque ($\Lambda = 10.75$), hence a larger accretion velocity. The pitch angle is defined as $\arcsin(-B_\phi/B_p)$ and the opening angle as $\theta = \arccos(B_z/B_p)$. In the ideal MHD region ($z(a) \geq 0.2r_o$), the magnetic field configuration and the velocity field are the same.

whereas dynamical quantities verify

$$
\begin{aligned}
&\rho_A \frac{\mu_o \Omega_o^2 r_o^2}{B_o^2} = \kappa^2 \\
&\frac{u_{p,A}}{\Omega_o r_o} = \frac{\lambda^{1/2}}{\omega_A} \\
&\left.\frac{u_p}{\Omega r}\right|_A = \frac{1}{\omega_A(1-g_A)}
\end{aligned}
\tag{52}
$$

where both the opening angle θ_A and the amount g_A of current available at the Alfvén surface ($I_A/I_{SM} = g_A(1+2\sigma_{SM}^{-1}) \simeq g_A$) are only functions of κ, λ and ω_A (Appendix A). Thus, the three jet parameters impose both the location of the Alfvén surface and the whole jet behaviour.

As a consequence, if different sets of disc parameters (ε, $\alpha_m, \mathcal{P}_m, \chi_m$) provide the same set of jet parameters (κ, λ, ω_A), then one gets identical jet configurations from different discs. The reason why this occurs lies in the resistive MHD conditions prevailing inside the disc. Thus, as long as there is no theory fixing the parameters for MHD turbulence, this situation remains.

We illustrate this property by showing in Fig. 6 the main characteristics of two jets with roughly (to whithin 10%) the same jet parameters. The first one (solid line) is launched from a dissipative disc with straight magnetic field lines, described by ($\varepsilon, \alpha_m, \mathcal{P}_m, \chi_m$) = (0.1,1.8,1, 0.139) and releasing 34 % ($\Lambda = 1.95$) of the total mechanical power. The resulting jets have (κ, λ,ω_A) = (7 10^{-3},65,1.56). The second one (dashed line) is launched from a weakly dissipative disc with bent magnetic field lines, $(\varepsilon, \alpha_m, \mathcal{P}_m, \chi_m) = (0.1, 0.945, 1, 0.366)$ and releasing only 8.5% ($\Lambda = 10.75$) of the mechanical power as radiation. In this case, the resulting set of jet parameters are almost the same, namely $(\kappa, \lambda, \omega_A) = (7.8\ 10^{-3}, 58, 1.63)$. However, a computation of a "real" MAES requires more parameters. Indeed, one must also specify the mass M_* of the central object, both inner (r_i) and external (r_e) radii where the MAES is established and the accretion rate $\dot{M}_{ae}$ at the external radius. While for most astrophysical objects, the central mass and accretion rate can be quite severely constrained, the radial extension of a MAES remains unknown. This is related to the amount of available magnetic flux, which must be assumed a priori. Thus, if one specifies the same accretion rate, a larger value of Λ (larger magnetic torque) gives rise to a larger accretion velocity, hence a smaller density at the disc midplane. This has several consequences that could be used to discriminate between these two solutions: (1) less dense discs can be potentially optically thin for the same accretion rate (FP95); (2) the ratio of the jet kinetic power to the disc luminosity is different; (3) different absolute values of the disc magnetic field (μ or B_o) therefore of the jet plasma density (ρ_A). In Fig. 7, we show the cross sections of two MAES producing the same jets, namely with same velocities, density stratification and magnetic field configuration. This was accomplished by imposing the same density at the disc midplane, which implies a different accretion rate.

To summarize, quasi-identical jet configurations can indeed be obtained from different discs. However, physical values such as accretion rates (or jet density) and ratio of disc luminosity to jet kinetic power, would be different. Thus, there is an one to one correspondance between a disc and its (cold) jets.

3.5. Comparison with other steady-state models

The main assumptions in the work presented here are: (1) discs are Keplerian and the launching zone is extended, (2) jets are cold. Thus, all models of jets from accretion discs obtained with these two basic assumptions should verify our analytical constraints.

Self-similar jets were already obtained by BP82, Wardle & Königl (1993) and Li (1995). Basically, our solutions are compatible with theirs, but we obtained a much smaller parameter space. In particular, they were able to obtain jets with huge magnetic lever arms λ and correspondingly small mass fluxes κ. While BP82 did not treat the disc, Wardle & Königl (1993) replaced mass conservation with the prescription $\rho u_z = Constant$ and Li (1995) imposed a static vertical disc structure. A correct treatment of the disc vertical equilibrium shows that large magnetic lever arms produce an overwhelming magnetic pressure squeezing the disc and forbidding any steady-state solution (see F97 for more details).

As in BP82, the jets found in this paper always undergo a recollimation, until the FM critical point is met. This systematic asymptotic behaviour is strongly influenced by the chosen self-similar geometry (F97). Nevertheless, using exactly the same self-similar ansatz, Contopoulos & Lovelace (1994) and more recently Ostriker (1997) did found jets with differ-

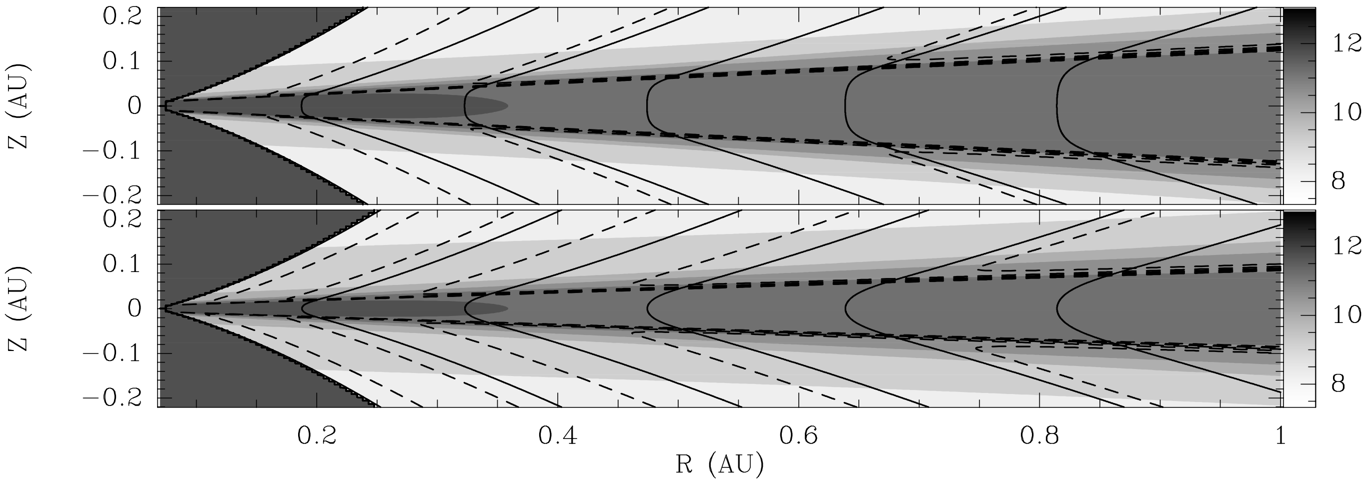

Fig. 7. Poloidal cross-section of two MAES driving jets with the same normalized jet parameters as in Fig. 6, around a one solar mass protostar. Poloidal magnetic field lines are displayed in solid lines, streamlines in dashed lines and number density ($\log_{10}(n_H/\mathrm{cm}^{-3})$) is shown in greyscale, from 12 to 7 by 1. In the upper model, the accretion rate, chosen to be $\dot{M}_{ae} = 10^{-7} M_\odot/yr$, is provided by both the turbulent viscous torque and the magnetic torque due to the jet. As a result, 34% of the accretion power is released as radiation. In the lower model, the magnetic torque due to the jet is dominant (only 8.5% of the power is radiated away), hence providing a higher accretion velocity. For the same plasma density at the disc midplane as in the upper model, one gets an accretion rate of $3.83\ 10^{-7} M_\odot/yr$.

ent behaviours. They were able to find jets with either an oscillating pattern or reaching a cylindrical collimation. This is possible only by varying the magnetic flux distribution in the disc, namely for $\beta > 1$. However, disc-driven jets must follow the scaling $\beta = 3/4 + \xi/2$ (FP95) where the trans-Alfvénic constraint imposes $\xi < 1/2$. Thus cold jets with $\beta > 1$ do not match the boundary conditions imposed by Keplerian accretion discs.

To our knowledge, only Li (1996) produced magnetically-driven jets from a Keplerian disc with straight magnetic field lines inside. In his model, ambipolar diffusion is the source of diffusivity in a quasi-neutral disc, whereas accretion is solely produced by the magnetic torque due to the jet (no turbulent "viscous" torque). Thus, almost no power is radiated by the disc and $\mathcal{P}_m << 1$. However, his solution displayed $\mu << 1$, thereby allowing a high mass loss rate from the disc (weak magnetic compression). This is outside our parameter range where we found μ to be always of order unity. This discrepancy might arise from the different set of equations used. In particular, Li (1996) did not use the induction equation for the magnetic field, but assumed instead frozen-in ions and got the magnetic field behaviour through the prescribed vertical dependency of the coupling coefficient.

4. Summary and concluding remarks

We investigated the full parameter space of cold, non-relativistic, magnetized accretion ejection structures (MAES). A generalization of previous works (FP95, F97) has been made by taking into account a radial transport of angular momentum in the disc. This turbulent transport is assumed to arise from MHD instabilities triggered inside the disc. As a consequence, a cold MAES is characterized by four local parameters: the disc aspect ratio ε, the strength of the MHD turbulence α_m, the magnetic Prandtl number $\mathcal{P}_m$ and the turbulent dissipation anisotropy χ_m.

Using self-similar solutions, we were able to obtain continuous solutions, from the disc midplane to super-Alfvénic jets. The parameter range where cold solutions are possible is quite narrow: $10^{-3} \leq \varepsilon < 0.3$, $0.3 \leq \alpha_m < 3$, $0 \leq \mathcal{P}_m \lesssim 4$ and $10^{-3} < \chi_m < 1$. Inside this parameter space, both dissipative and weakly-dissipative discs are allowed. A dissipative disc releases a significant fraction of the accretion (mechanical) power as radiation at its surfaces. The magnetic torque is comparable to the turbulent "viscous" torque ($\Lambda \sim 1$). A weakly dissipative disc transfers most of the available power to an MHD Poynting flux, which is finally converted into jet kinetic power. Only a small fraction of the power is radiated away, and the magnetic torque is dominant ($\Lambda \gg 1$).

The importance of the dissipation is controlled by the properties of the MHD turbulence. But since a MAES must also magnetically drive cold winds, there is a link between these properties and jet launching conditions. This crucial relation is expressed in Eq. (21), namely

$$\Lambda \sim \frac{\chi_m/\varepsilon}{\alpha_m \alpha_v} \ . \tag{53}$$

Dissipative discs require $\chi_m \sim \varepsilon$, i.e. anisotropic magnetic diffusivities for thin discs. In other words, turbulence must lead to a dissipation of the toroidal field stronger than for the poloidal field. Dissipative MAES require either α_m or α_v bigger than unity. Thus, if one demands those parameters to be always smaller than unity, only weakly dissipative MAES are possible. We believe this is a general result for steady-state structures. It arose from analytical considerations and is thus independent of our self-similar ansatz. However, it does depend on two assumptions, namely a Keplerian disc and cold ejection.

Applying these assumptions to an extended launching zone, we derived general analytical links between relevant jet parameters (κ, λ and ω_A) and disc parameters. The most powerful relation, linking accretion to ejection, is Eq. (33)

$$\omega_A \sim m_s \frac{\Lambda}{1+\Lambda} \frac{\lambda^{3/2}}{\lambda - 1} \frac{\sin(\phi_A - \theta_A)}{\sin \phi_A} \tag{54}$$

which must be bigger than (but of the order of) unity. The larger ω_A, the larger the maximum jet radius. The above equation, coming from magnetic flux conservation, shows how this jet parameter is intimately related to the accretion process ($m_s = u_o/\Omega_K h$). This is quite obvious for a dominant magnetic torque, where the toroidal field at the disc surface is large. Would the "viscous" torque be dominant ($\Lambda \ll 1$), the sonic Mach number would be very small, $m_s \sim \alpha_v \varepsilon$. The constraint $\omega_A > 1$ would then require a huge magnetic lever arm from a thin disc. It is doubtful such solutions could exist, the disc being probably too much squeezed by the magnetic pinching force. Another alternative would be a tremendously high viscosity parameter $\alpha_v \sim \varepsilon^{-1}$, which is unphysical.

Two biases were nevertheless introduced in our numerical solutions. The first one arises from the geometry itself. Indeed, self-similar solutions are only valid for MAES settled on a large radial extension. As a consequence, a cylindrical rather than a spherical geometry is already imposed. This fixes the Alfvén surface, so that $z_A \sim r_A$ is always verified (ϕ_A between $20°$ and $50°$), hence making gravity negligible there. As a result, it can be shown that Λ must be larger than (or of the order of) unity. Therefore, no cold solution with $\Lambda \ll 1$ on a large radial extension can be found. However, note that such a small value of Λ would have tremendous implications on the MHD turbulence parameters χ_m, α_m and α_v.

The second bias was already found by PP92. A class of jets described with the same parameters in all magnetic surfaces become super-fast magnetosonic (in the conventional sense, $u_p > V_{FM}$) and then recollimate toward the axis. Self-similar jets from Keplerian discs fall into this category (F97). A realistic modelling of self-collimated jets must therefore be done outside a self-similar framework. However, the interrelations between the underlying disc and its jets (links between invariants) should be used. Ouyed et al. (1997) performed numerical simulations of MHD jets from Keplerian accretion discs, using the disc as a boundary condition. They obtained solutions that recollimate also toward the axis and produce fast MHD shocks. Knots are episodically formed at a fixed position and, once formed, propagate further down the jet. They proposed that this recollimation and unsteady knot production is realized whenever the toroidal magnetic field is large enough, namely when $N = B_\phi^2/2\mu_o \rho u_p^2 > 1$ at the disc surface. It is remarkable that our calculations of cold MAES satisfy this criterion.

We showed that there is an univocal link between an accretion disc and its jets. But interpreting observations is quite tricky, since it depends on assumptions about jet emission properties (Cabrit et al. 1999). However, global considerations can already provide some constraints on theoretical models, like the ratios $2\dot{M}_j/\dot{M}_a$ ($= \xi \ln r_e/r_i$) and P_{jet}/P_{rad} ($= \Lambda$). If Λ is found to be larger than unity, then the portion of the disc responsible for mass ejection (from r_i to r_e) should consistently produce a hole in the spectral energy distribution. Moreover, since we found an ejection efficiency ξ which lies typically around 0.01, mass fluxes could provide another measure of the MAES's radial extension. Young stellar objects produce jets with typical velocities of 300 to 500 km/s. If we assume that these jets are produced by a MAES located after the corotation radius, too high velocities are obtained. This is because the magnetic lever arm is quite large. Thus, models with smaller lever arms λ should be sought. However, this is impossible for cold jets within a self-similar framework.

Another alternative would be that the emission is dominated by the external radii of the MAES. In that case, only the outer velocities would be inferred from the observational data, thus underestimating asymptotic velocities. To settle this question, one needs to solve the energy equation along the jet and produce synthetic emission maps (Garcia et al., in preparation).

As said previously, we trust our results are quite general for Keplerian accretion discs launching cold jets from a large radial extension. The next generalization is to relax the assumption of cold ejection. Indeed, even if plasma pressure may have no dynamical role in jet equilibrium, it might produce non-negligible effects on the ejection mechanism itself. In particular, since the vertical equilibrium at the disc surface may be deeply modified, different mass loads and/or initial jet velocities are expected. The presence of hot coronae is quite commonly argued for accretion discs, from both theoretical (Galeev et al. 1979) and observational (e.g. Kwan 1997) grounds. Introducing a hot corona is consistent with the presence of a turbulent "viscous" torque. Indeed, such a torque probably arises from 3D MHD turbulence in the disc. Numerical simulations tend to show the formation of a magnetized, hot medium above the disc (Stone et al. 1996). In our model, a small fraction of the mechanical power liberated by this torque could be converted into coronal heating. This work is currently under progress.

Finally, it has been argued that advection dominated accretion flows could also produce self-collimated jets (see Narayan & Yi 1995, Soria et al. 1997). These are quite promising configurations, especially in the context of galactic and extragalactic compact objects. In this paper, we mainly focused our attention on thin (even slim) accretion discs. But our framework, with the further development of a hot corona, will allow us to investigate the behaviour of flows of that kind.

Acknowledgements. We would like to thank Guy Pelletier for stimulating discussions and helpful comments about the manuscript.

Appendix A: Physical constraints at the Alfvén point

In Grad-Shafranov equation (28) evaluated at the Alfvén point ($m = 1$), the most difficult term to figure out is the density gradient. To solve this problem, we consider the function $g = 1 - \Omega/\Omega_*$, which can be written

$$g = \frac{m^2}{m^2-1}\left(1 - \frac{r_A^2}{r^2}\right) . \tag{A1}$$

Taking the gradient of this equation and noting that $m^2 = \rho_A/\rho$ provides

$$\nabla \ln\left(\frac{g}{\rho_A}\right) = \frac{1}{\rho_A - \rho}\left(\frac{2r_A}{r^2}(\nabla r - \nabla r_A) + \nabla\rho - \nabla\rho_A\right) \tag{A2}$$

Thus, the regularity condition at the Alfvén point is

$$\nabla \ln \rho|_A = \nabla \ln \rho_A + \frac{2}{g_A r_A}(\nabla r_A - \mathbf{e}_r) \tag{A3}$$

where we made the assumption that jet invariants are the same in every magnetic surface. Inserting the regularity condition in the Grad-Shafranov equation (28) provides

$$\cos\theta_A = \frac{g_A r_A^2 \eta^2}{2B_{p,A}}\left[\frac{d\mathcal{E}}{da} + (1-g_A)\Omega_* r_A^2 \frac{d\Omega_*}{da} + g_A\Omega_*\frac{d\Omega_* r_A^2}{da} + \frac{2V_{Ap,A}^2}{g_A r_A}\frac{dr_A}{da} + \frac{V_{Ap,A}^2}{2}(1+\omega_A^2 g_A^2)\frac{d\ln\rho_A}{da}\right] \tag{A4}$$

This is a general result as long as the jet parameters are the same for every magnetic surface. In the case of radial self-similarity, it takes the much simpler form

$$\cos\theta_A = \frac{g_A}{2}\frac{\kappa\lambda^{3/2}}{\omega_A}\frac{\Omega_o}{\Omega_*}\left[\omega_A^2\left(\frac{\alpha_4}{2}g_A^2 + 2g_A + \frac{3}{2}\left\{\frac{1}{\lambda} - 1\right\}\right) + \frac{\alpha_4}{2} + \frac{2}{g_A}\right] \tag{A5}$$

where $\alpha_4 = 2\beta - 3$. Thus, the opening angle at the Alfvén point depends only on g_A, κ, λ and ω_A. Now, Bernoulli equation evaluated at the Alfvén surface provides

$$g_A^2 = 1 - \frac{3}{\lambda} - \frac{1}{\omega_A^2} + \frac{2}{\lambda^{3/2}(1 + z_A^2/r_A^2)^{1/2}} . \tag{A6}$$

Note that the last expression is valid for every model of disc-driven, cold jets. If the magnetic lever arm is very small ($\lambda < 3$), then the fastness parameter must be large, namely $\omega_A > 2$, even taking into account the gravity term ($g_A^2 > 0$).

Appendix B: Shape of the Alfvén surface and ω_A

The definition (32) of ω_A can be written, using the definition of the mass load κ,

$$\omega_A = \kappa\lambda^{1/2}\sqrt{\frac{\Omega_o}{\Omega_*}\frac{B_o}{B_{p,A}}} . \tag{B1}$$

If we assume the Alfvén surface to be conical, as in radial self-similar works or in some numerical simulations of disc-driven jets (Sakurai 1987, Krasnopolsky et al. 1999), then the magnetic flux conservation provides

$$\frac{B_o}{B_{p,A}} = \frac{\Omega_o}{\Omega_*}\lambda\frac{\sin(\phi_A - \theta_A)}{\sin\phi_A} \tag{B2}$$

where ϕ_A is the angle between the Alfvén surface and the vertical axis ($z_A/r_A = \cot\phi_A$ in a self-similar solution). Injecting this result in Eq. (B1) gives

$$\omega_A \simeq \kappa\lambda^{3/2}\frac{\sin(\phi_A - \theta_A)}{\sin\phi_A} , \tag{B3}$$

since $\Omega_o \simeq \Omega_*$ in thin discs. Our solutions always displayed $1 < \omega_A < 2$ and never higher values. The reason for that behaviour is hidden in Grad-Shafranov equation (A5), which imposes a highly non-linear link between ω_A and the opening angle θ_A. Nevertheless, we observe that θ_A increases with ω_A (see e.g. Fig. 6 in F97), while the above expression of ω_A shows that it should decrease for increasing θ_A. Thus, the jet transverse equilibrium seems to impose here some feedback, forbidding high values for ω_A. As a consequence, Bernoulli equation prohibits small values of the magnetic lever arm λ.

Smaller magnetic lever arms could however be obtained for different geometries. To illustrate this, we examine a spherical Alfvén surface, in the particular case where magnetic field lines are almost straight (Najita & Shu 1994). In this case, one has

$$\frac{B^+}{B_{p,A}} \simeq \frac{\lambda}{\varepsilon^2\sin^2\theta_A}$$
$$\omega_A \simeq \kappa\frac{\lambda^{3/2}}{\varepsilon^2\sin^2\theta_A}\frac{B_o}{B^+} \tag{B4}$$

where B^+ is the poloidal magnetic field at the disc surface. Large values of ω_A with small magnetic lever arms are allowed here because of the large dilution of the magnetic flux.

References

Balbus, A.S., Hawley, J.F., 1991, ApJ, 376, 214
Blandford, R.D., Payne, D.G., 1982, MNRAS, 199, 883 (BP82)
Cabrit, S., Ferreira, J., Raga, A.C., 1999, A&A, 343, L61
Chan, K.L., Henriksen, R.N., 1980, ApJ, 241, 534
Contopoulos, J., Lovelace, R.V.E., 1994, ApJ, 429, 139
Ferreira, J., Pelletier, G., 1993, A&A, 276, 625 (FP93)
Ferreira, J., Pelletier, G., 1995, A&A, 295, 807 (FP95)
Ferreira, J., 1997, A&A, 319, 340 (F97)
Galeev, A.A., Rosner, R. , Vaiana, G.S., 1979, ApJ, 229, 318
Hartigan, P., Edwards, S., Ghandour, L., 1995, ApJ, 452, 736
Heyvaerts, J., Norman, C., 1989, ApJ, 347, 1055
Khanna, R., Camenzind, M., 1994, ApJ, 435, L129
Königl, A., 1989, ApJ, 342, 208
Kwan, J., 1997, ApJ, 489, 284
Lery, T., Heyvaerts, J., Appl, S., Norman, C.A., 1998, A&A, 337, 603
Lery, T., Henricksen, R.N., Fiege, J.D., 1999, A&A, 350, 254
Li, Z.-Y., 1995, ApJ, 444, 848
Li, Z.-Y., 1996, ApJ, 465, 855
Livio, M., 1997 ASP conference Series, Vol 121, Wickramasinghe, T., Ferrario, L., Bicknel, G.V. (eds.), p 845
Krasnopolsky, R., Li, Z.Y., Blandford, R., to appear in ApJ (Dec 1999). Draft version at astro-ph/9902200
Michel, F.C., 1969, ApJ, 158, 727
Najita, J., Shu, F.H. 1994, ApJ, 429, 808
Narayan, R., Yi, I., 1995, ApJ, 444, 231
Ostriker, E.C., 1997, ApJ, 486, 291
Ouyed, R., Pudritz, R.E., Stone, J.M., 1997, Nature, 385, 409

Pelletier, G., Pudritz, R.E., 1992, ApJ, 394, 117 (PP92)
Pouquet, A., Frisch, U., Leorat, J., 1976, J. Fluid Mech., 77, 321
Pudritz, R.E., 1981, MNRAS, 195, 897
Rüdiger, G., Elstner, D., Stepinski, T.F., 1995, A&A, 298, 934
Rutten, R.G.M., van Paradijs, J., Tinbergen, J., 1992, A&A, 260, 213
Sakurai, T., 1987, PASJ, 39, 821
Serjeant S., Rawlings, S., Lacy, M., Maddox, S.J., Baker, J.C., Clements, D., Lilje, P.B., 1998, MNRAS, 294, 494
Shakura, N.I., Sunyaev, R.A., 1973, A&A, 24, 337
Soria, R., Li, J., Wickramasinghe, D. T., 1997, ApJ, 487, 769
Stone, J.M., Hawley, J.F., Gammie, C.F., Balbus, A.S., 1996, ApJ, 463, 656
Torkelsson, U., Brandenburg, A., 1994, A&A, 283, 677
Wardle, M., Königl, A., 1993, ApJ, 410, 218
Yoshizawa, A., Yokoi, N., 1993, ApJ, 407, 540